Linear Optimal Theory Applied to Active Structural Bending Control

RALPH E. SMITH* AND EVAN L. S. LUM†
Autonetics Division of North American Rockwell Corporation, Anaheim, Calif.

To improve ride qualities and structural fatigue life of high-performance aircraft, control of structural flexing is desirable. Linear optimal control via the root-square locus was employed to design a simple, effective bending-control system for four XB-70 coupled longitudinal bending modes. The weighted sum of the mean-square differential angular acceleration and the control surface position was minimized for random wind-gust inputs. Approximation of frequency response characteristics of high-order optimal compensations led to a suboptimal mechanization (fixed-parameter, third-order transfer function with a programmed gain) which produced nearly optimal performance for three diverse low-altitude flight cases. The rms differential angular acceleration was reduced by a factor of 5 for a control expenditure of approximately 13°/sec rms elevon rate per fps of rms wind-gust velocity. Changed vehicle parameters for a fourth flight case require different sensor locations for effective control. Extensive design data show correlation of performance with plant gain and performance-index weighting factors, indicating a potential for predesign prediction of results. Comparable performance is provided by simple, uncompensated feedbacks for some cases, but stability margins are lower than for the near-optimal systems.

Nomenclature

C_u = general plant output resulting from control action
D = open-loop response‡ of variable to be controlled
FC = flight case
G_1 = plant transfer function, including servo actuation and airframe dynamics
G_c = compensation transfer function
K_1 = gain factor§ of transfer function G_1
K_p = scalar weighting factor on mean-square control error in optimal performance index
n_{zp} = normal acceleration at pilot station
$\dot{q}_D$ = differential angular pitch acceleration
s = Laplace operator
w_g = wind-gust velocity
X = s^2, transform variable for root-square locus
Z = transfer function consisting of $\{\Phi_{DD}(s)\}^+$
δ_E = elevon angle
σ_{wg} = rms wind-gust velocity
ω = frequency, rad/sec

Introduction

HIGH-PERFORMANCE air vehicles tend toward high length-to-thickness external shapes for aerodynamic reasons. This leads to increased structural flexibility with accompanying lower natural frequencies of structural flexing. Because of the gust-input characteristic of high energy at low frequency, and increased coupling of bending modes with the low-frequency, rigid-body motion, the structural flexing is increased, which leads to a rough ride and possible reduced structural-fatigue life. Thus, it is desirable to control vehicle bending action.

Most of the past bending-control work has been directed toward passive control, where the bending signals sensed by body-mounted instruments are eliminated by filtering or cancellation from the normal feedback paths. The passive approach has produced, for example, a "gyro blender" scheme for cancellation of the effects of a single mode and tracking filters for cancellation of multiple modes. In contrast, the objective of this study was to control actively the bending mode so that the response to a disturbance or control input would be reduced with respect to the open-loop response. It is recognized that a form of active control may result from a design process based on a passive viewpoint, but the active viewpoint was employed here.

Stochastic wind-gust inputs were utilized in this study since they provide the highest energy input at the bending frequencies. Because stochastic inputs are used, the frequency domain formulation of the problem was employed rather than the time domain. This formulation also seemed to have the advantage of producing most directly the desired polynomial-ratio form of compensation.

The theoretical formulation and solution are essentially those presented by Chang,[1] where the basis is Wiener filter theory with an added Newton constraint. Chang's root-

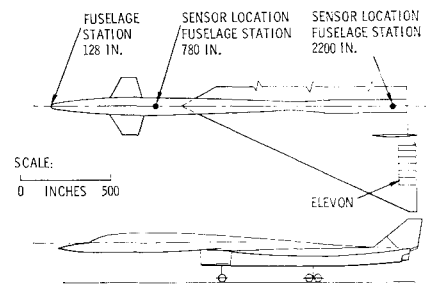

Fig. 1 General XB-70 configuration.

Presented as Paper 66-970 at the AIAA Third Annual Meeting and Technical Display, Boston, Mass., November 29–December 2, 1966; submitted December 12, 1966; revision received September 28, 1967. The results reported were derived from a research effort sponsored and directed by the Air Force Flight Dynamics Laboratory, Research and Technology Division, Air Force Communications System, U.S. Air Force, Wright-Patterson Air Force Base, under Contract AF33(615)-3133, and conducted jointly with the Los Angeles Division, North American Aviation Inc.

* Member of Technical Staff, Advanced Engineering, Data Systems Division.

† Member of Technical Staff, Advanced Engineering, Data Systems Division.

‡ Time and Laplace transform functions are distinguished by the context or the equation where used.

§ Gain factors are defined for coefficients of the highest power of the numerator and for denominator polynomials equal to unity.

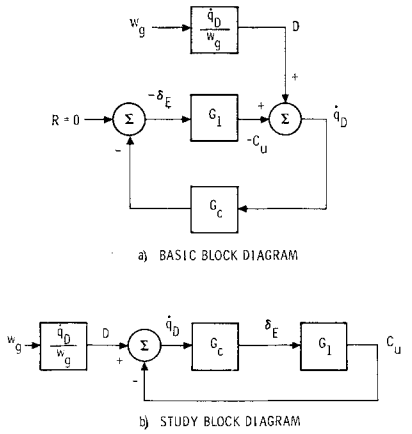

Fig. 2 General optimal study block diagrams.

square locus is used to facilitate solution of the spectral factorization problem. Recent work by Rynaski and Whitbeck[2] was helpful in understanding the variations in both the linear optimal theory and its application.

The immediate objective of the subject study was to determine if a simple, practical system design could be derived from linear optimal-control theory. This paper presents initial results of that investigation. More detailed information[3] has been published.

Problem Approach

Study Model and Control Variables

The study vehicle was the XB-70 having the configuration shown in Fig. 1. The segmented elevons were employed for control. The vehicle dynamical representation consists of the linearized pitch, plunge, and four coupled bending-mode equations, all containing quasi-steady aerodynamic coefficients, and wind-gust terms. A first-order servo-actuator dynamic lag with a break frequency of 20 rad/sec was included. The widely used gust-power spectral density,

$$\Phi_{gg}(\omega) = \sigma_{wg}^2 \left(\frac{L}{\pi V_0}\right) \frac{[1 + 3(L\omega/V_0)^2]}{[1 + (L\omega/V_0)^2]^2} \tag{1}$$

having the mean-square value

$$\sigma_{wg}^2 = \int_0^\infty \Phi_{gg}(\omega) d\omega \tag{2}$$

was approximated by

$$\Phi_{ggA}(\omega) = \frac{2\sigma_{wg}^2}{3^{1/2}} \left(\frac{L}{\pi V_0}\right) \frac{1}{\{1 + [L\omega/(3)^{1/2}V_0]^2\}} \tag{3}$$

where L is the scale of turbulence = 600 ft and V_0 is the vehicle velocity (fps). The factor $2/3^{1/2}$ in the approximation was selected to produce equal rms values for both spectra. The effect of other control systems such as the stability augmentation system was omitted in this first study since it was desired only to use a representative form of plant.

A feedback variable $\dot{q}_D$, the difference of the outputs of two widely separated angular accelerometers, was selected to provide a bending signal that is independent of rigid-body motion. Differential angular acceleration is

$$\dot{q}_D = \sum_{i=1}^{4} (\phi'_{ix1} - \phi'_{ix2})\ddot{\eta}_i + \dot{q}_{x1} - \dot{q}_{x2} \tag{4}$$

where ϕ'_{ix1} is the slope of the ith bending mode at station x_1 of the forward instrument location (x_2 is the station location of the aft instrument) (deg/ft), $\ddot{\eta}_i$ is the acceleration of the ith mode in generalized coordinate (ft/sec^2), and $\dot{q}_{x1}$ is the rigid-body angular acceleration at the forward instrument location (deg/sec^2).

It is apparent that the two rigid-body terms cancel for equal gain factors on the instrument outputs. Only angular measurement instruments have the advantage of thus eliminating both translational and rotational rigid-body motion. Angular acceleration was selected over rate in preliminary studies.

Although the over-all objective is to reduce linear acceleration at the pilot's station and that acceleration has not been related to the selected feedback variable $\dot{q}_D$, it is reasonable to assume that if successful bending control is achieved, the contribution of body bending to the rms pilot acceleration will be reduced. Hence, total acceleration at the pilot's station will be reduced significantly since the addition of bending effects more than doubles the total rms acceleration.

The basic block diagram is shown in Fig. 2a, where the plant (or vehicle dynamics) to be controlled is G_1, the disturbance input to the control loop is D, $\dot{q}_D$ is the measured state variable, and the compensation G_c is to be determined.

Essential Theory and Definitions

The block diagram for application of the theory is shown in Fig. 2b, which is a simple rearrangement of Fig. 2a to a conventional controller diagram form. The theory for application to that diagram was adopted from Chang,[1] and the following is offered to aid in relating the optimal solutions from the source to the present application.

First, it is noted the subject theory was developed for a servomechanism, whereas the desired control design is for a regulator. The difference is simply one of inputs and sensed variables. For the theoretical development, the input is a command and the sensed variable is the controlled variable. For the present application, the input is a disturbance and the sensed variable is a resultant error that the control is designed to reduce.

The second major difference is that the development of the optimal equation employed was for deterministic inputs and for minimum-phase plants (plants having no right-half-plane (RHP) zeros), whereas the present application was to optimize for stochastic inputs and for some nonminimum-phase plants. As noted by Chang (Ref. 1, Chap. 4), the mathematics are essentially the same for both cases. The modification for nonminimum-phase plants from Chang's Chap. 4 was superimposed on the optimal solution of Chap. 2.

Some key relations are now listed in outline form. The specific solution is limited to a stable plant with a single control input and a single feedback variable. Of course, multiple inputs and outputs may be combined according to some other criteria and the over-all combination viewed as a single-input single-output plant. Plant zeros in the RHP are acceptable. It should be emphasized that limitations just mentioned as well as some of the solution characteristics are not inherent to optimal control, but only to the solution form employed here.

The plant transfer function is

$$G_1 \triangleq \frac{K_1 N_1}{D_1} \triangleq \left(K_1 \prod_{j=1}^{m} (s - z_j) \Big/ \prod_{i=1}^{n} (s - p_i)\right) \tag{5}$$

The disturbance response characteristic is

$$Z \triangleq \{\Phi_{DD}(s)\}^+ \triangleq K_z N_z / D_z \tag{6}$$

where $\phi_{DD}(s)$ = power spectral density of D, the open-loop response of the variable to be controlled, and $\{F\}^+$ indicates the product of the LHP factors of the numerator and denominator of F.

The performance index form to be minimized is

$$K_p\langle \dot{q}_D^2 \rangle + \langle \delta_E^2 \rangle$$

where the angular brackets indicate time average and K_p is

a scalar weighting factor to be selected during the design.

The optimal closed-loop transfer function is

$$F_{OK} = (1/YZ)[Z/\bar{Y}]_+ \triangleq C_u/D \tag{7}$$

$$F_{OK} = \frac{N_1 D_z}{K_{\bar{Y}Y} N_Y N_z}\left[\frac{N_z \bar{N}_1}{D_z \bar{N}_Y}\right]_+ \tag{8}$$

where

$$Y \triangleq (K_{\bar{Y}Y})^{1/2}\{\bar{D}_1 D_1 + K_p K_1^2 N_1 \bar{N}_1\}^+/N_1 \triangleq (K_{\bar{Y}Y})^{1/2} N_Y/N_1 \tag{9}$$

$$\left[\frac{N_z \bar{N}_1}{D_z \bar{N}_Y}\right]_+ = \sum_{j=1}^{k} \frac{A_j}{s - \alpha_j} \triangleq \frac{K_R N_R}{D_z} \tag{10}$$

$[F]_+$ indicates partial-fraction expansion of F about LHP poles of F, α_j is one of the k roots of D_z, A_j is the residue of function in brackets at the root α_j, and the bar in $\bar{Y}$ indicates function $Y(s)$ with s replaced by $-s$, or $Y(-s)$ where the denominator of Y equals the numerator polynomial of G_1.

In this form given in (9), Y applies to plants with or without zeros in the RHP. The function N_Y is derived from the root-square locus.

The closed-loop optimal form, useful in design evaluation, is

$$q_D/D \triangleq 1/(1 + G_c G_1) = (N_Y N_z - K_0 N_1 N_R)/N_z N_Y \tag{11}$$

where

$$K_0 = (-1)^{n-m} K_p K_1^2 K_R \qquad n > m \tag{12}$$

$$K_0 = K_p K_1^2 K_R/(1 - K_p K_1^2) \qquad n = m \tag{13}$$

The optimal compensation is

$$G_c = K_c D_1 N_R/(N_Y N_z - K_0 N_1 N_R) \tag{14}$$

where

$$K_c = K_0/K_1 \tag{15}$$

Note that if the order of $N_Y N_z$ is equal to the order of $N_1 N_R$, the coefficient of the highest power of s in the denominator of (14) is $(1 - K_0)$.

Root-square locus computation of N_Y is

$$D_1 \bar{D}_1 + K_p K_1^2 N_1 \bar{N}_1 = 0 \tag{16}$$

This equation is the factorization problem to be solved. It is handled as follows:

$$(-1)^{n-m} K_p K_1^2 \prod_{j=1}^{m} (X - Z_j) \Big/ \prod_{i=1}^{n} (X - P_i) = -1 \tag{17}$$

where $X = s^2$, $P_i = p_i^2$, and $Z_j = z_j^2$.

The root-square locus, an ordinary root locus based on (17) with K_p as the variable gain factor, is

$$Y\bar{Y} = K_{\bar{Y}Y} \prod_{i=1}^{n} (X - Q_i) \Big/ \prod_{j=1}^{m} (X - Z_j) \tag{18}$$

where Q_i is one of the roots from the root-square locus for a particular value of K_p, and

$$N_Y = \prod_{i=1}^{n} (s - q_i)$$

where $q_i = \pm(Q_i)^{1/2}$. The sign is selected to satisfy the equation $N_Y = \{D_1 \bar{D}_1 + K_p K_1^2 N_1 \bar{N}_1\}^+$.

Simplification of the Optimal Design

Application of the previous equation for the optimal compensation to bending-control problems reveals some unfortunate characteristics. First, it is very complex for realistic plants. It is evident that the compensation order is generally greater than that of the plant. Further, the compensation numerator order may be higher than that of the denominator. In addition, the numerator contains the plant denominator, and identical cancellation of at least part of the plant denominator roots is required. For an optimal design based on the complete Z function, rather than on an approximation of Z, the compensation denominator contains the denominator of the open-loop plant transfer function. Therefore, cancellation within the compensation simplifies it, and the extensive cancellation in a mechanization of an optimal mechanization would be obviated.

If a form of optimal-control system involving cancellation of plant poles by the compensation were mechanized, a question could logically be raised regarding the system controllability, although the question is generally not relevant for the simplified system. One of the manifestations of Kalman's complete controllability and observability is that a system transfer function from the control input to any output of interest contains no cancellable factors.[4] Yet, the new open-loop system transfer function $G_c G_1$ would contain a large set of cancellable factors. Although no formal investigation was made, a few comments on physical considerations are appropriate. If an oscillation of one of the plant modes were initiated, it would be difficult to control, because the input to the compensation would be greatly attenuated by the compensation numerator factor at the mode frequency. A tentative conclusion is that the effect would not be very significant for the subject problem, since the response to initial conditions, including store drops, does not last long with respect to the total flight time. Most oscillations arise from disturbance inputs, so if a closed-loop response is produced which attenuates these input effects, the system would appear satisfactory. A hurried computer check of these concepts on an optimal bending compensation of low effectivity was inconclusive. At any rate, the simplification process employed here generally produced no exact cancellation of plant poles.

Additional characteristics encountered were that the compensation might be either nonminimum phase or unstable, in spite of the fact that stability of the closed-loop optimal system is guaranteed. Unstable compensation is impractical even though it produces a stable closed-loop system, and fortunately it has not appeared except for a few early design cases.

The first step in simplification of the compensation is the reduction of the order of the input Z such that it only approximates the original frequency-response characteristic. Then, an optimal compensation is derived for the simplified input. Finally this compensation is similarly simplified by approximation in the frequency domain. For the case of no RHP zeros (RHP poles are excluded for both Z and G_c), the gain vs frequency characteristic was approximated experimentally. If RHP zeros exist, as is sometimes the case for the compensation, then the phase angles must also be considered. Gain asymptote sketches on the gain-frequency curve were considered to be the simplest way to approximate the function. For the suboptimal compensations thus derived, the system stability, which is guaranteed for the optimal solution, must be checked.

Deliberate changes in the weighting of the Z function for a certain range of frequencies have also been made for system considerations such as the derivation of a compensation without an active integrator ($1/s$ in the transfer function), or the modification of the interaction of the bending control with other control functions.

Design Procedure

The over-all design procedure is now summarized in the following steps with added helpful notes:

1) Simplify Z function by approximating the gain-frequency characteristic.

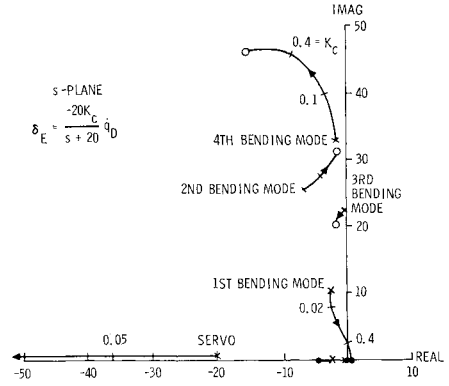

Fig. 3 Root locus for simple gain feedback, *FC* 1.

2) Obtain N_Y, which forms part of the optimal closed-loop loop poles, for a particular K_p by the root-square locus method.

a) Square the plant gain and roots.

b) Compute a root locus using the square quantities from 2a. The K_p should be increased until the poles approach the vicinity of the zeros for maximum control effect. An exception may be when a zero is near the negative real axis of the root-square locus which causes the optimal pole to approach instability. For all other cases, the loci are repelled from regions of marginal stability (vicinity of the negative part of the real axis on the X plane). This fact allows an easy check for the proper sign of gain in the root-locus computation.

c) Take the square root of the roots and retain those in the LHP. These are part of the optimal closed-loop poles. (An obvious alternate to steps 2a through 2c is to compute a root locus directly from $K_p\bar{G}_1\bar{G}_1 = -1$ in the s plane and retain the LHP poles).

3) Obtain N_R and K_R by the residue method and summation of fractions.

4) Compute the optimal closed-loop gain, K_o, and the numerator of (11). (A root locus routine is convenient for simultaneously combining and factoring the numerator).

5) Obtain a gain-frequency plot of the closed-loop transfer function $\dot{q}_D/D$, to check the computational procedure and design effectivity. The gain should be less than unity at the frequencies of the peaks in Z. This closed-loop transfer function is optimal for the simplified Z.

6) Compute the optimal compensation gain K_c and reduce the order of the optimal compensation by approximating the gain-frequency characteristics. If nonminimum-phase functions are involved, it is necessary to also give attention to the phase characteristic. A plot of poles and zeros on the s plane is sometimes helpful to determine if pole-zero combinations may be omitted.

7) Check the degree of suboptimal system stability by an open-loop frequency response using the suboptimal compensation. The order of the closed-loop system is increased with respect to the open-loop plant.

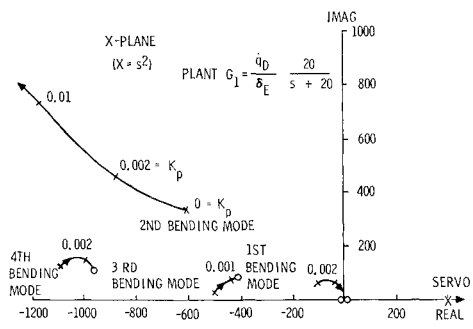

Fig. 4 Root-square locus, *FC* 1.

Table 1 Flight-case conditions

FC	Mach no.	Altitude	Weight
1	0.9	0	Heavy
2	0.9	0	Light
3	0.4	0	Heavy
4	0.4	0	Light

8) For evaluation purposes, compute the rms values of the controlled output, control effort, and other variables of interest.

XB-70 Application

System Design

The design approach for suboptimal systems briefly outlined previously was applied to the problem of designing a bending-control compensation for the symmetric modes of the XB-70. Four low-altitude flight cases having rather extreme environmental conditions were used, as shown in Table 1. Vehicle dynamics[5] included the first four coupled-structural modes. It was assumed that two angular accelerometers were located at stations 780 and 2200, and the measured differential angular acceleration was fed to all of the elevon segments through the compensation and a first-order servo lag at 20 rad/sec. For simplicity in the design process, the servo was considered as part of the plant, leading to minimization of the mean-square command to the servo rather than control surface position. Design examples have shown that substitution of actual surface position, or even rate, in the performance index for servo command showed no difference in control efficiency. Instrument dynamics were neglected. The wind-gust approximate spectra of (3) were utilized in the system design and performance elevation. Complete Z functions, rather than the approximations of Z, were used for system evaluation.

Figures 3-8 and Fig. 10 show typical data plots of interest in the design for one flight condition (*FC* 1). Figure 3 presents a root locus for the case of a simple gain feedback to indicate the general characteristics of the bending mode dynamics.

The root-square locus and the corresponding plot of optimal closed-loop poles are shown in Figs. 4 and 5, respectively. The greatest degree of control is achieved for the highest values of K_p. However, since high K_p values place very low relative weighting on control effort, some intermediate value produces the most efficient control. The best criteria for selection of K_p are still under study.

Although rigid-body motion is not sensed directly, Figs. 3 and 5 indicate that high bending-control gain places new, complex closed-loop roots near the short-period frequency of approximately 3 rad/sec. Thus, the low-frequency response characteristics may be affected by the bending-control system because of coupling in the vehicle dynamics.

Figure 6 presents an example approximation of the Z function of the XB-70 symmetric-bending response. The over-

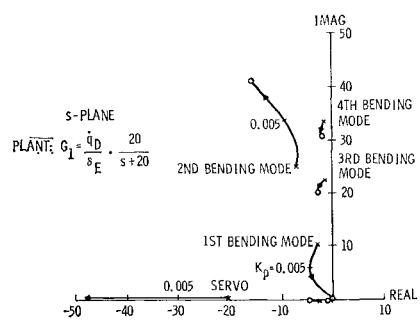

Fig. 5 Optimal closed-loop roots, *FC* 1.

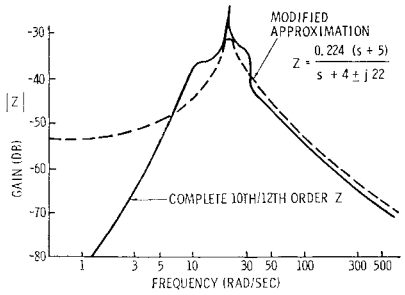

Fig. 6 Approximation for *Z*: Airframe bending due to wind-gust input, *FC* 1.

all gain level is arbitrary since it cancels out in the solution. The wide gain deviation at low frequency was the result of a deliberate modification to produce improved system characteristics. In this case, the change moved a compensation pole at zero to about -1, thus resulting in a more practical compensation with insignificant change in performance. Figure 7 presents the approximation for the compensation which is optimal for the foregoing simplified and modified input. This approximation, as will be noted later, was made to fit *FC*'s 2 and 3, as well as *FC* 1.

The closed-loop $\dot{q}_D/D = 1/(1 + G_cG_1)$ gain vs frequency produced by the preceding compensation is presented in Fig. 8. This is the gain characteristic that modifies the bending response to disturbance inputs and also the normal vehicle response to control surface commands. For example, if the pitch-rate response with the bending-control loop open is q/δ_{Ec}, then the response with the bending loop closed is $(q/\delta_{Ec})[1/(1 + G_cG_1)]$. Note that the low-frequency characteristic is not affected much by the bending-control loop. Based on Fig. 8, the simplified compensation would be expected to produce a general reduction of the bending input which is comparable with that of the more complex "optimal" ("optimal" is used to designate a system which is optimal for a simplified input) compensation. The suboptimal closed-loop gain to be applied to the inputs is lower than that for the optimal compensation at some frequencies and higher at others, resulting in approximately equal rms closed-loop performance. The $\dot{q}_D/D$ gain-frequency curve is used during design to check the computational results. For an effective design, this curve has the shape of the inverted image of the approximate Z, such as shown in Fig. 6.

The simplified compensation was selected for the candidate optimal designs, which produced approximately 80% reduction in rms $\dot{q}_D$ for three flight conditions. *FC* 4 was omitted because it represents an unusual and difficult plant, which may be eliminated by improved selection of sensor locations. The selection criterion for the compensation was the simplest way to produce the best over-all approximate fit for the frequency-response curves of the optimal compensations based on the simplified inputs for *FC*'s 1–3. The result is the general suboptimal compensation

$$G_c = \frac{K_c(s + 16)(s^2 + 6s + 130)}{(s + 1.5)(s^2 + 30s + 1450)} \tag{19}$$

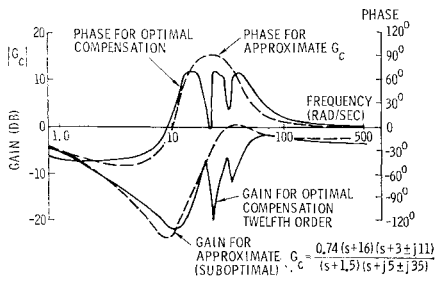

Fig. 7 Approximation of optimal compensation frequency response, *FC* 1.

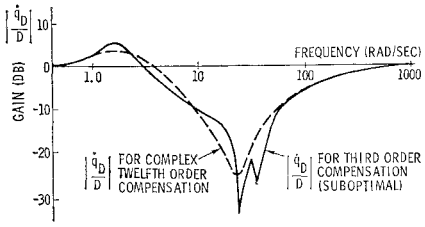

Fig. 8 Closed-loop function $\dot{q}_D/D$ frequency response, *FC* 1.

for *FC*'s 1–3, where $K_c = 0.74, 0.14$, and 1.4, respectively. A block diagram of a possible mechanization is shown in Fig. 9. The required gain change could be programmed or adjusted adaptively. The variation indicated in K_c is approximated by the inverse of M_{δ_E}, the maximum-pitch angular acceleration per unit elevon deflection as in the moment equation $\dot{q} \cong M_{\delta_E}\delta_E$.

Figure 10 shows a typical open-loop, gain-phase plot using the suboptimal compensation with the plant for *FC* 1. The stability margins are shown in Table 2. Although the optimal design process assures stability, it is noted that the optimal design for the difficult *FC* 4 had a rather low stability margin. This margin could be improved by a design for a lower K_p value with little loss in performance.

System Performance

Results of optimal designs based on approximate inputs are presented to show the effects of changing plant and design parameters. The suboptimal system mechanization was based on the highest K_p values shown for each flight case. Performance figures were essentially the same for the approximate, simplified compensations, as for the optimal compensations. As noted subsequently, the stability and/or control power are generally different if the bending reduction is the same. Some discrepancies are introduced by the fact that the optimal case is actually suboptimal for the complete, complex input which is used to evaluate both optimal and simplified designs.

Figure 11 shows that the rms differential angular acceleration $\dot{q}_D$ is reduced by approximately 80% for *FC*'s 1–3. A reduction of approximately 20% is effected for *FC* 4. These summary data are plotted vs the product of plant gain K_1 and $K_p^{1/2}$, where K_p is the weighting factor in the performance index. This parameter $|K_1|K_p^{1/2}$, which is a portion of the optimal system loop gain, was selected by analysis of the design data.

The basic cause of different performance for *FC* 4 is that the plant contains 5 RHP zeros, whereas the others contain either 1 or no RHP zeros. It is known that for nonminimum-phase plants, a performance limit exists. It is also known that the sensor locations should generally be selected to avoid RHP zeros. Hence, it is assumed that if the sensor locations had been optimized, results would be generally more uniform. Recent studies involving different airframe dynamics have supported this assumption.

Control-surface rms rates were used for system evaluation and comparison because the rate was more critical with respect to normal limiting values than was the surface position. Figures 11 and 12 indicate that the best results for all four flight conditions are produced with an expenditure

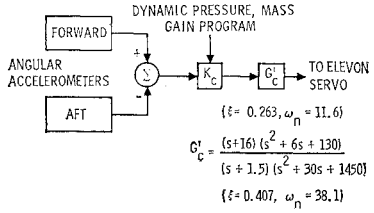

Fig. 9 Example of finalized XB-70 symmetric bending-control system design.

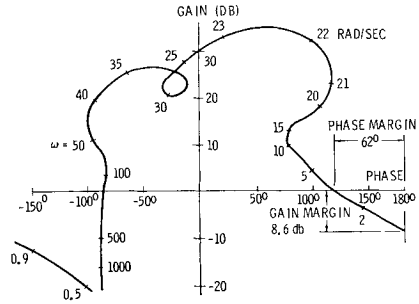

Fig. 10 Gain-phase for suboptimal system, third-order compensation, *FC* 1.

of rms elevon rate of about 13°/sec per fps rms wind gust. This value is high with respect to typical available rates. It is possible, by improved sensor locations and lower K_p values, to reduce the rms elevon rate to a reasonable level while retaining acceptable bending-reduction performance. It is noted that the use of an elevon segment consisting of one-third the control surface area and located midway between the elevon inboard and outboard extremities, required an rms rate of approximately three times the rate for the entire elevon to effect the same percent reduction in rms $\dot{q}_D$. A curve representing designs for this elevon segment plotted on Fig. 11 also indicates that the selected design parameter $|K_1|K_p^{1/2}$ correlates it with the other cases rather closely. Figure 12 shows a relatively consistent variation of rms surface rate as a function of the design parameter, except for maverick *FC* 4.

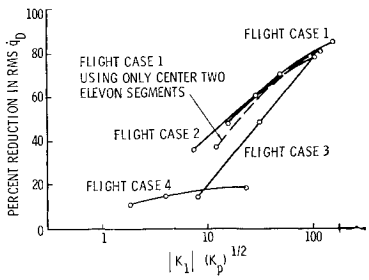

Fig. 11 Percent reduction rms $\dot{q}_D$ vs $|K_1|(K_p)^{1/2}$.

Figure 13 summarizes the reduction in rms acceleration at the pilot's station. The selected K_p values produced reductions ranging from 14 to 45% for *FC*'s 1–3. The correlation of normal acceleration with design parameters is not as good as for $\dot{q}_D$ because of the varying mode characteristics and the fact that n_{zp} is not the feedback variable. It should be noted that the choice of feedback sensors obviates effective control of the contribution of rigid-body motion to rms n_{zp}. For *FC* 4 the total rms acceleration is actually increased slightly. However, the final rms acceleration for unity rms wind gust is only 0.0267 *g*/fps, which is lower than the highest closed-loop value of 0.033 *g*/fps for other flight cases. It was observed that the trends of reduction of n_{zp} are more closely related to the reduction in $\dot{q}_D$ for the cases where the original plant to be controlled has no RHP zeros. It is apparent that the greatest deviation in the n_{zp}

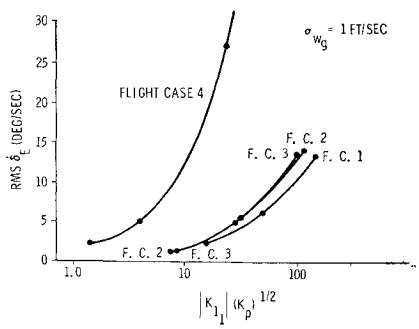

Fig. 12 rms elevon rate $\dot{\delta}_E$ vs $|K_1|(K_p)^{1/2}$.

Table 2 Summary stability margins

	Optimal		Suboptimal, 3rd-order G_4	
Flight case	Gain, db	Phase, deg	Gain, db	Phase, deg
1	11	62	8.6	62
2	∞	73	∞	74
3	∞	77	∞	65
4	3.5	60	...	...

trends in Fig. 13 from the trends for $\dot{q}_D$ in Fig. 11 occurred for *FC*'s 1 and 4, each of which contained RHP zeros.

The system sensitivity to plant and control-system parameter variations has yet to be evaluated. However, some inherent insensitivity to variations of parameter is suggested by the fact that separate suboptimal compensations for three diverse flight conditions could be approximated by a single transfer function with variable gain which produces good performance and stability.

Optimal, Suboptimal, and Simple System Comparison

Finally, the system performance is compared with that of simple systems without compensation, where either differential angular acceleration or rate are fed back directly as servo commands, e.g., $\delta_{Ec} = K_c \dot{q}_D$. Figures 14a–14c highlight the major points; *FC* 2 was omitted because it is very similar to *FC* 1. Closed-loop rms $\dot{q}_D$ and q_D are plotted vs rms δ_E. The greatest control "efficiency" is indicated by a down-left position on the graph. Figure 14 indicates the superiority of $\dot{q}_D$ feedback over q_D. The latter actually increases closed-loop rms $\dot{q}_D$ for *FC* 1 as did $\dot{q}_D$ feedback for the very difficult *FC* 4. The optimal and suboptimal designs are always superior to the simple feedback cases. Although the differences are not as great as might be hoped, the optimal systems use less control effort for a given level of rms $\dot{q}_D$, and produce greater reduction in $\dot{q}_D$ for a given level of δ_E. The optimal design showed some improvement for *FC* 4, whereas the simple $\dot{q}_D$ system increased the bending.

Another disadvantage of the simple system is that the stability is much lower. For example, to retain 6-db gain margin on *FC* 1, the minimum rms $\dot{q}_D$ for the simple system would be 100% higher than that for the best optimal system shown. For the cases checked, if the suboptimal system shows a greater reduction in $\dot{q}_D$ than the optimal system, this reduction is accomplished by higher rms elevon rate and/or a reduction in degree of stability. Figure 14a also shows a one-point optimal design for a case where $\langle \dot{\delta}_E^2 \rangle$ replaced $\langle \delta_E^2 \rangle$ in the performance criterion. No difference in performance is indicated.

An increasing difference between optimal systems and those with simple gain feedback is shown in Figs. 14b and 14c. This increasing difference generally implies a compensation less amenable to simplification. Thus, the greater difference in performance would be achieved only by increased complexity of suboptimal compensation.

Conclusions

Differential angular acceleration is generally more effective for bending-mode control than is differential angular rate.

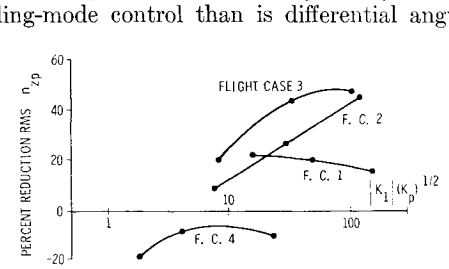

Fig. 13 Percent reduction rms n_{zp} vs $|K_1|(K_p)^{1/2}$.

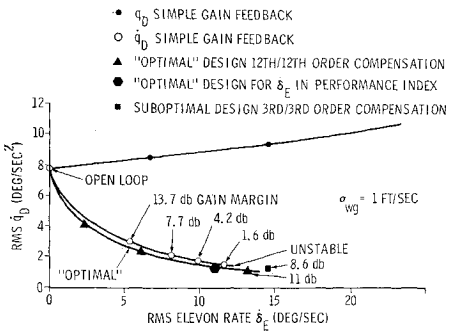

a) For *FC* 1

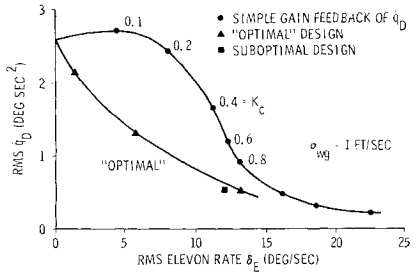

b) For *FC* 3

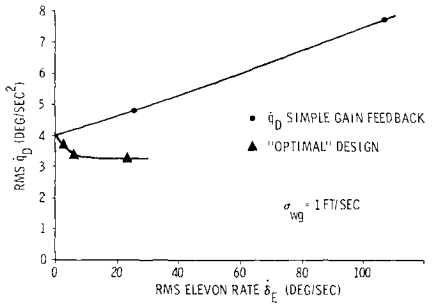

c) For *FC* 4

Fig. 14 Comparison of optimal design to simple gain feedback.

Differential angular-acceleration feedback to a single control surface with simple gain feedback is effective for many cases considered. However, suboptimal systems consistently produce less rms bending for a given control effort, or use less control effort for the same bending reduction. For the cases checked, the suboptimal systems also exhibit better stability margins.

Linear optimal control formulated to produce series polynomial-ratio compensation, operating on one feedback variable and controlling one input variable, sometimes results in a compensation which identically cancels most of the plant poles. The optimal compensation may be unstable, may contain zeros in the right-half-plane, and may have a numerator of higher order than the denominator.

Linear suboptimal control as outlined here is useful as a design basis for active bending control. The optimal compensation may be greatly simplified by approximating the gain-frequency characteristic of stochastic inputs and the total frequency-response characteristic of the optimal compensation designed for the simplified input. The final suboptimal compensation exhibits approximately the same effectivity as the most complete optimal compensation in reducing the rms error. However, it is generally accomplished with the expenditure of additional control power and/or the final suboptimal system exhibits lower stability margins. The closed-loop suboptimal system may be simplified or made more compatible with other system considerations by deliberate modification of the disturbance input spectrum.

For XB-70 plant dynamics containing four coupled longitudinal-bending modes, the rms total differential bending signal due to stochastic wind-gust inputs is reduced 80% or by a factor of 5, using single aerodynamic force points at the aft end of the vehicle for three flight conditions. Reductions in rms vertical acceleration at the pilot's station ranged from 14 to 45%. Elevon control surface rms rate of approximately 13°/sec per fps of rms wind gust is required. A fixed-parameter, third-over-third-order compensation network combined with a variable-gain factor produces the foregoing good results. Four flight conditions involving extremes of Mach number and weight at low altitude could apparently be covered if improved sensor location produced well-behaved plants having one or less zeros in the right-half-plane, which are no more difficult to control than *FC* 1.

Implicit information indicating low sensitivity to vehicle parameters is contained in the fact that a single third-order network combined with a variable gain approximation for three different complex networks provides good performance and stability. For well-behaved plants studied here, the rms level of the controlled variable or differential bending, and control surface rate are relatively well correlated with the parameter $|K_1|(K_p)^{1/2}$, where K_1 is the plant-gain factor and K_p is a weighting factor in the performance index. Thus, at least for similar plants, the results are approximately predictable at the start of the design. Because of rate limit considerations, the rms control-surface rate appears more critical than rms surface position in the bending-control system design. Substitution of power servo output position or rate for power servo commanded position in the performance index for limited examples resulted in a negligible change in performance.

References

[1] Chang, S. S. L., *Synthesis of Optimum Control Systems*, McGraw-Hill, N.Y., 1961, Chaps. 2 and 4.

[2] Rynaski, E. G. and Whitbeck, R. F., "The Theory and Application of Linear Optimal Control," Rept. IH-1943-F-1, Cornell Aeronautical Lab.; also Rept. AFFDL-TR-65-28, Oct. 1965, Air Force Flight Dynamics Lab.

[3] Lum, E. L. and Smith, R. E., "Linear Optimal Control Theory and Angular Acceleration Sensing Applied to Active Structural Bending Control on the XB-70," C5-1574.8/33, April 5, 1966, Autonetics; published in revised form as Rept. AFFDL-TR-66-88, May 1967, Air Force Flight Dynamics Lab.

[4] Butman, S. and Sivan, R., "On Cancellations, Controllability and Observability," *Institute of Electrical and Electronics Engineers Transactions on Automatic Control*, Vol. AC-9, No. 3, July 1964, pp. 317–318.

[5] Wykes, J. H. and Mori, A. S., "An Analysis of Flexible Aircraft Structural Mode Control," Rept. AFFDL-TR-65-190, Part I, Dec. 1965, Air Force Flight Dynamics Lab.